


Article

Co-Immobilization of D-Amino Acid Oxidase, Catalase, and Transketolase for One-Pot, Two-Step Synthesis of L-Erythrulose

Daria Świętochowska ^{1,2} , Aleksandra Łochowicz ¹, Nazim Ocal ³, Loredano Pollegioni ⁴, Franck Charmantray ³, Laurence Hecquet ³ and Katarzyna Szymańska ^{5,*}

¹ Department of Organic Chemistry, Bioorganic Chemistry and Biotechnology, Silesian University of Technology, 44-100 Gliwice, Poland

² Biotechnology Center, Silesian University of Technology, B. Krzywoustego 8, 44-100 Gliwice, Poland

³ Institut de Chimie de Clermont-Ferrand, CNRS Auvergne Clermont INP, Université Clermont Auvergne, F-63000 Clermont-Ferrand, France

⁴ Department of Biotechnology and Life Sciences, Università degli Studi dell'Insubria, 21100 Varese, Italy

⁵ Department of Chemical Engineering and Process Design, Silesian University of Technology, 44-100 Gliwice, Poland

* Correspondence: katarzyna.szymanska@polsl.pl

Abstract: Here, we present an immobilized enzyme cascade in a basket-type reactor allowing a one-pot, two-step enzymatic synthesis of L-erythrulose from D-serine and glycolaldehyde. Three enzymes, D-amino acid oxidase from *Rhodotorula gracilis* (DAAO_{Rg}), catalase from bovine liver (CAT), and transketolase from *Geobacillus stearothermophilus* (TK_{gst}) were covalently immobilized on silica monolithic pellets, characterized by an open structure of interconnected macropores and a specific surface area of up to 300 m²/g. Three strategies were considered: (i) separate immobilization of enzymes on silica supports ([DAAO][CAT][TK]), (ii) co-immobilization of two of the three enzymes followed by the third ([DAAO+CAT][TK]), and (iii) co-immobilization of all three enzymes ([DAAO+CAT+TK]). The highest L-erythrulose concentrations were observed for the co-immobilization protocols (ii) and (iii) (30.7 mM and 29.1 mM, respectively). The reusability study showed that the best combination was [DAAO + CAT][TK], which led to the same level of L-erythrulose formation after two reuse cycles. The described process paves the way for the effective synthesis of a wide range of α-hydroxyketones from D-serine and suitable aldehydes.

Keywords: co-immobilization; one-pot, two-step cascade; monolithic silica pellets; modular production system of L



Citation: Świętochowska, D.; Łochowicz, A.; Ocal, N.; Pollegioni, L.; Charmantray, F.; Hecquet, L.; Szymańska, K. Co-Immobilization of D-Amino Acid Oxidase, Catalase, and Transketolase for One-Pot, Two-Step Synthesis of L-Erythrulose. *Catalysts* **2023**, *13*, 95. <https://doi.org/10.3390/catal13010095>

Academic Editors: Anna Gancarczyk and Agnieszka Ciemięga

Received: 17 November 2022

Revised: 15 December 2022

Accepted: 21 December 2022

Published: 3 January 2023

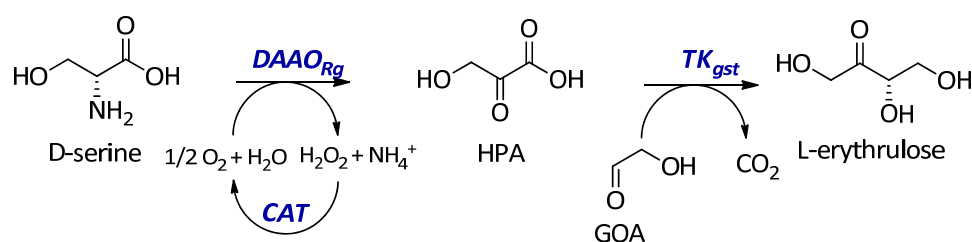


Copyright: © 2023 by the authors. Licensee MDPI, Basel, Switzerland. This article is an open access article distributed under the terms and conditions of the Creative Commons Attribution (CC BY) license (<https://creativecommons.org/licenses/by/4.0/>).

1. Introduction

Enzyme cascades are a promising system for the multistep biocatalytic synthesis of rare sugars with unique biological activities [1–5]. Most reports describe the use of free enzymes in small reaction volumes, and their effective use beyond the proof-of-concept stage or the use of enzyme cascades efficiently at a larger scale is challenging. Their complexity necessitates a proper balance of a large set of interdependent reaction variables such as temperature and pH. One major hurdle in making enzyme cascades operational is the management of the recycling of the whole enzyme ensemble for multiple rounds of conversion [6]. Traditionally, enzyme recycling is handled through their immobilization. Such technology is well developed for single enzymes but is not as advanced for enzyme cascades [7–15]. Commonly, the immobilization of enzyme ensembles can be achieved by their separate immobilization on individual support particles or by the co-immobilization of all the enzymes on the same support. The fundamentals, advantages, and disadvantages of these immobilization strategies have been presented in review papers [16–20]: it was noted that co-immobilization favours the channelling effect, whereas separate immobilization facilitates enzyme-specific optimization of activity or stability.

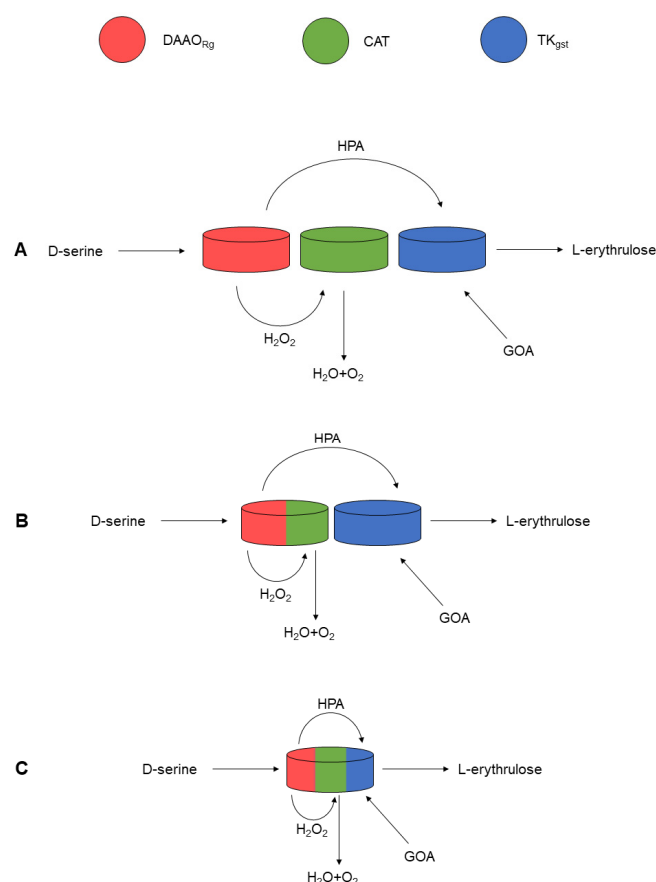
Different types of enzyme supports have been used for enzyme immobilization: polymeric supports [21,22], carbon nanotubes [23–25], or inorganic supports including porous silicon oxides [7,8,26–28]. Recently, monolithic silica supports have been developed, characterized by an open structure of interconnected macropores and a specific surface area of up to 300 m²/g. These supports take the form of cones or cylinders with an equivalent grain diameter of 2–4 mm, so they can be successfully used in basket reactors [26,28]. Biocatalysts based on monolithic supports were shown to exhibit significantly higher activity than catalysts based on commercial silica gels, even though both types of supports had the same specific surface area [26]. An additional advantage of monolithic supports was that they can be regenerated after enzyme deactivation [26]. In this study, as a proof of principle, we investigated the co-immobilization of three enzymes, D-amino acid oxidase (DAAO), catalase (CAT), and transketolase (TK) for the synthesis of L-erythrulose from two model substrates, D-serine and glycolaldehyde (GOA). These enzymes have already been immobilized separately using different techniques [9–14,29,30], but never jointly on the same type of support for a convergent application. The key step was catalysed by TK for the transfer of a ketol group from an α -ketoacid (hydroxypyruvate, HPA) as a donor to an aldehyde as an acceptor. The major advantage of this strategy is the use of HPA, making the reaction irreversible through the release of CO₂ (Scheme 1). The TK-catalysed reaction leads to (3S)-hydroxyketones through stereoselective C–C bond formation.



Scheme 1. Coupling of DAAO_{Rg} and TK_{gst} for L-erythrulose synthesis from D-serine and glycolaldehyde (GOA).

These properties lend TK_{gst} a chemical synthetic potential that makes it an attractive biocatalyst for the synthesis of chiral α -hydroxyketones valuable as pharmaceuticals, food additives, or various chemicals [3]. In addition, while the common TK sources were mesophilic enzymes [31,32], thermostable TKs were recently described [33–35], particularly TK from *Geobacillus stearothermophilus* (TK_{gst}) offering long-term stability up to 60 °C [36,37]. However, the main hurdle is the synthesis and the instability of HPA. To circumvent this limitation, the in situ generation of this compound was described from D-serine. An efficient route catalysed by DAAO from *Rhodotorula gracilis* (DAAO_{Rg}) coupled with CAT for hydrogen peroxide dismutation and with TK_{gst} in the presence of a suitable aldehyde as an acceptor was recently reported (Scheme 1) [4].

Here, we considered three strategies for enzyme immobilization: (i) separate immobilization of each enzyme on the silica support [DAAO][CAT][TK] (Scheme 2A), (ii) co-immobilization of two of the three enzymes, followed by the third [DAAO+CAT][TK] (Scheme 2B), and (iii) co-immobilization of all three enzymes [DAAO+CAT+TK] (Scheme 2C). This approach allowed us to assess the impact of the substrate channelling effect on L-erythrulose concentration assuming enzyme immobilization on a support with an unusually open pore structure.



Scheme 2. Three combinations of immobilized DAAO_{Rg}, CAT and TK_{gst}. Separate immobilization of each enzyme [DAAO][CAT][TK] (A), co-immobilization of DAAO_{Rg} and CAT and separate immobilization of TK_{gst} [DAAO+CAT][TK] (B), co-immobilization of all three enzymes [DAAO+CAT+TK] (C).

2. Results and Discussion

One of the most frequently used methods for the enzyme immobilization of enzymes is their covalent binding to support. The durability of the connection usually makes the biocatalysts obtained in this manner highly stable [38–40]. In this work, enzymes were covalently bound to monolithic silica pellets (Figure 1) functionalized with amino groups using glutaraldehyde as a linker.

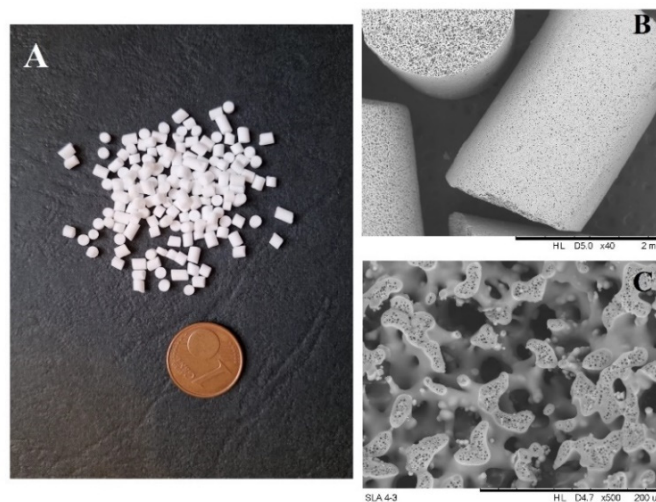


Figure 1. Monolithic silica pellets (A) and their SEM images (B,C).

We started our study by determining the optimal operating temperatures of the two key enzymes (DAAO_{Rg} and TK_{gst}) after their immobilization (Figure 2), as the temperature is a significant variable affecting the activity and stability of immobilized enzymes. For this purpose, each of the enzymes was immobilized on a separate support and the enzymatic activities were then determined in the temperature range 25–80 °C by HPLC monitoring of the product formation (HPA from D-serine for DAAO_{Rg} or L-erythrulose from HPA and GOA for TK_{gst}). Immobilized DAAO_{Rg} (3.3 mg of DAAO_{Rg}/g_{silica}) and TK_{gst} (8.3 mg of TK_{gst}/g_{silica}) exhibited maximum activities at 40 °C and 50 °C, respectively. These values were closed to those obtained for free enzymes [36,37,41].

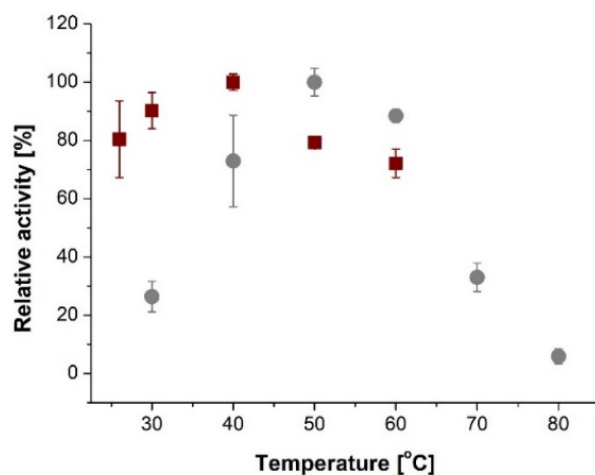


Figure 2. Temperature profile of DAAO_{Rg} (■) and TK_{gst} (●) immobilized on monolithic silica pellets functionalized with amino groups; relative activity defined as an activity at a certain temperature to the highest activity (at 40 °C for DAAO_{Rg} and 50 °C for TK_{gst}). DAAO_{Rg} conditions: D-serine (50 mM) in Tris-HCl (0.5 M, pH 7.5), in the presence of O₂, DAAO_{Rg} immobilized on silica pellets modified with amino groups (0.03 g of biocatalyst), free catalase powder (0.1 mg), 26–60 °C, 500 rpm. TK_{gst} conditions: HPA (50 mM), GOA (50 mM), ThDP (0.1 mM), MgCl₂ (1 mM), TK_{gst} immobilized on silica pellets modified with amino groups (0.018 g of biocatalyst, 0.15 mg of protein), pH 7.0, 30–80 °C, 500 rpm.

The long-term stability of each immobilized enzyme was also investigated after different incubation times (0, 24, 48, 72, and 96 h) and at specific temperatures (26, 30, and 40 °C) considering the temperature profiles of both enzymes obtained previously (Figure 2). At 26 and 30 °C, the immobilized DAAO_{Rg} remained stable for approximately 100 h (Figure 3A) showing a significant improvement of the stability over the free enzyme (Supporting Information, Figure S1). At 40 °C its activity decreased slightly over time (Figure 3A). Immobilized TK_{gst} showed stability in all tested temperatures (Figure 3B). Surprisingly, there was an increase in activity (for both enzymes) during the time, which may be due to conformational changes in the protein structure after immobilization. CAT used in this study was a commercial enzyme from Sigma-Aldrich (Poznan, Poland) for which an optimum operating temperature of 20–40 °C was determined [42,43].

To perform the cascade with the three immobilized enzymes DAAO_{Rg} should produce HPA from D-serine, which is subsequently converted to L-erythrulose using TK_{gst} as a catalyst in the presence of GOA (Scheme 1). Owing to the instability of HPA in aqueous solutions [3–5], it is advisable to run both steps simultaneously. The process conditions must therefore be compatible with the stability of all the enzymes. Because DAAO_{Rg} undergoes slow deactivation at 40 °C (Figure 3A) in reported studies with immobilized enzymes, the maximum process temperature was 30 °C.

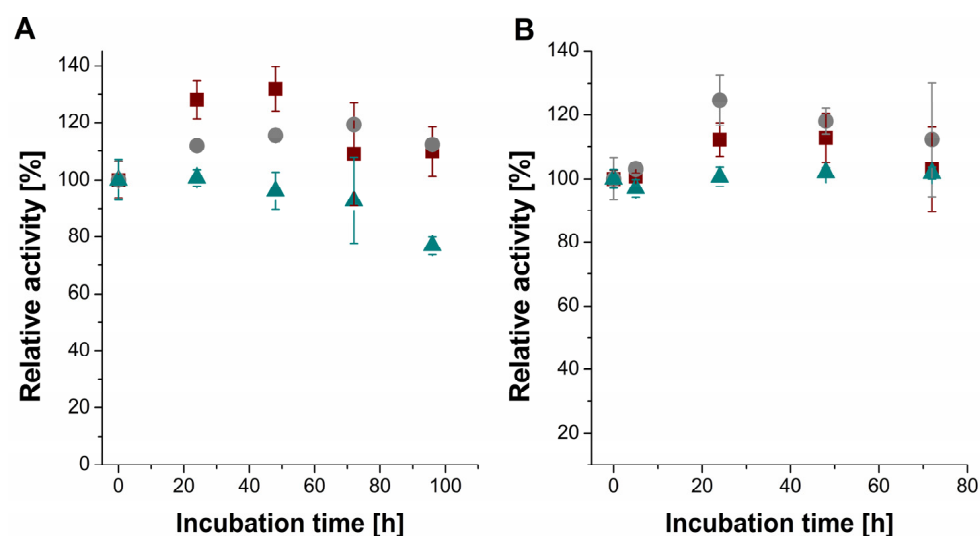


Figure 3. Long-term thermal stability of immobilized DAAO_{Rg} (A) and TK_{gst} (B). Enzymes were incubated in H₂O with cofactors ThDP (0.1 mM) and MgCl₂ (1 mM) at 26, (■) 30, (●) 40 °C (▲). The enzyme activity before incubation is 100%. DAAO_{Rg} reaction conditions: D-serine (50 mM) in Tris-HCl (0.5 M, pH 7.5), DAAO_{Rg} immobilized on silica pellets modified with amino groups (0.03 g of biocatalyst), free CAT in powder (0.1 mg), 26 °C, 500 rpm, in the presence of O₂. TK_{gst} reaction conditions: HPA (50 mM), GOA (50 mM), ThDP (0.1 mM), MgCl₂ (1 mM), TK_{gst} immobilized on amino-modified silica pellets (0.018 g of biocatalyst), pH 7.0, 50 °C, 500 rpm.

The next stage of the study was to determine the stability of the immobilized enzymes in subsequent reaction cycles. To detect the factors that could influence the final yield, the stabilities of immobilized DAAO_{Rg} and immobilized TK_{gst} were determined separately. Because H₂O₂ produced during the first stage can induce DAAO_{Rg} deterioration [4,11,29,30], CAT was also immobilized on the same support. DAAO_{Rg}/CAT and TK_{gst} immobilized independently showed very high stability after five consecutive process cycles each lasting 6 h (Figure 4). In view of these findings, we estimated that the immobilized enzymes were stable for at least one working week.

To evaluate the best conditions to develop the cascade reaction, three combinations of immobilized enzymes were considered (Scheme 2): enzymes separately immobilized on the silica supports [DAAO][CAT][TK] (Scheme 2A), co-immobilization of DAAO_{Rg} and CAT and separately immobilized TK_{gst} [DAAO+CAT][TK] (Scheme 2B), and co-immobilization of all three enzymes [DAAO+CAT+TK] (Scheme 2C). Almost the same amount of enzymes was used in the process (Table 1).

The lowest L-erythrulose concentration was obtained using enzymes immobilized separately on the supports [DAAO][CAT][TK] (Figure 5), despite the fact that in this case the slightly higher quantities of enzymes were recorded in the system (Table 1). In this case, HPA and H₂O₂ released by DAAO_{Rg} were not in close contact with the active site of CAT and TK_{gst} for which they are substrates (Scheme 2A). In addition, H₂O₂, not immediately transformed by CAT, could negatively influence DAAO_{Rg} activity. This presumably contributed to the lower L-erythrulose concentration compared to the other immobilized enzyme combinations [DAAO+CAT][TK] and [DAAO+CAT+TK]. Higher L-erythrulose concentrations were obtained for the other two immobilization protocols, [DAAO+CAT][TK] and [DAAO+CAT+TK] (Figure 5), showing that the proximity of CAT and DAAO_{Rg} had a positive effect on the formation of HPA and consequently on L-erythrulose synthesis.

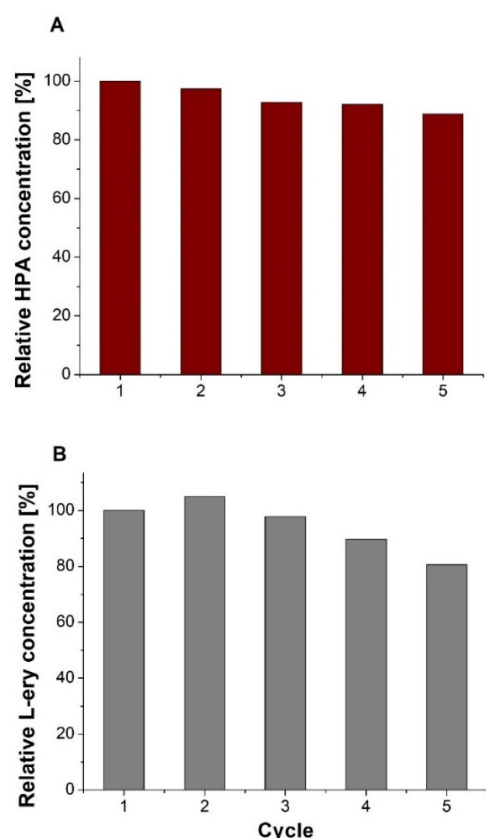


Figure 4. Recycling of co-immobilized DAAO_{Rg} and CAT (**A**) and immobilized TK_{gst} alone (**B**) at 30 °C. Conditions (**A**): D-serine (50 mM), ThDP (0.1 mM), MgCl₂ (1 mM), DAAO_{Rg} and CAT co-immobilized on amino-modified silica monolithic pellets (0.5 g of biocatalyst with immobilized 2 mg of DAAO_{Rg}, 4 mg of CAT), 30 °C, 400 rpm, in the presence of O₂, 6 h of each cycle. The enzyme activity after the 1st cycle is 100%. Conditions (**B**): HPA (50 mM), GOA (50 mM), ThDP (0.1 mM), MgCl₂ (1 mM), TK_{gst} immobilized on amino-modified silica monolithic pellets (0.5 g of biocatalyst with immobilized 6 mg of TK_{gst}), 30 °C, 400 rpm, 6 h of each cycle; 100% is the enzyme activity after the 1st cycle.

Table 1. Amounts of enzymes applied in different types of cascade.

Cascade	DAAO _{Rg} [mg]	TK _{gst} [mg]	CAT [mg]
[DAAO][CAT][TK] (Scheme 2A)	2.17	7.39	4.34
[DAAO+CAT][TK] (Scheme 2B)	1.71	7.40	3.80
[DAAO+CAT+TK] (Scheme 2C)	1.45	6.41	3.38

This result shows the importance of the substrate channelling effect [19] allowing a direct transfer of H₂O₂ to the active site of CAT avoiding its destructive effect on DAAO_{Rg}. Similar observations were made in the work of Mathesh et al. [44], where co-immobilization of glucose oxidase (GOD) and horse radish peroxidase (HRP) resulted in better substrate conversions compared to separate immobilisation of these enzymes. In the case of TK, this channelling effect was less significant since the two combinations [DAAO+CAT][TK] and [DAAO+CAT+TK] gave approximatively the same L-erythrulose yield. This could be explained by good mass transport between grains offered by the unique structure of the monolithic support (Figures 1 and 5). We note a slightly lower L-erythrulose concentration

when TK_{gst} was co-immobilized with DAAO_{Rg} and CAT (Scheme 2C), probably due to the slower reaction rate of TK_{gst} compared to DAAO_{Rg} or fewer bound enzymes (Table 1).

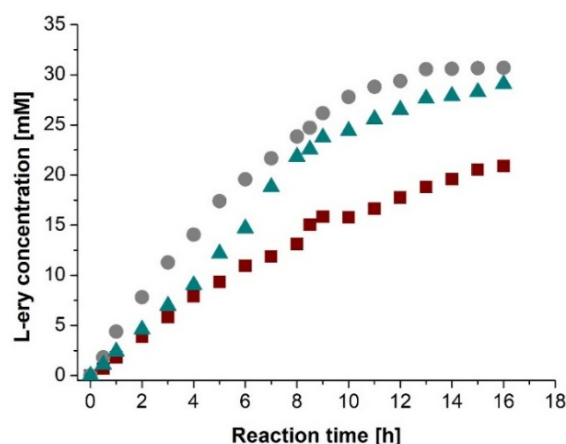


Figure 5. L-erythrulose (L-ery) synthesis by different combinations of immobilized enzymes: each enzyme separately [DAAO][CAT][TK] (■), [DAAO+CAT] together and [TK] separately (●) and the three enzymes together [DAAO+CAT+TK] (▲). Conditions: D-serine (50 mM), GOA (50 mM), ThDP (0.1 mM), MgCl₂ (1 mM), pH 7.0, 30 °C, 400 rpm, in the presence of O₂. pH was regulated by pH-stat for 16 h. The quantities of each enzyme are indicated in Table 1 (1 g of biocatalyst).

For biocatalytic applications particularly at the industrial level, the reusability of the catalysts is an important factor. Thus, for the best two combinations of catalysts [DAAO+CAT+TK] and [DAAO+CAT][TK], the overall efficiency of both enzymatic cascade systems was evaluated considering the L-erythrulose formation after each cycle. The best results were obtained with [DAAO+CAT][TK] (Figure 6), in line with the best efficiency of the system previously described (Figure 5), leading to the same level of L-erythrulose formation after two cycles (Figure 6), while [DAAO+CAT+TK] showed a complete loss of activity after the second cycle (Figure 7). The decrease in enzyme activity after the second or third cycles (Figures 6 and 7) were surprising considering that the activity of each enzyme immobilized in both systems tested separately with respective substrates exhibited very high stability and efficiency after five cycles (Figure 4A,B). Inhibition of DAAO_{Rg} by GOA over time is suspected (already mentioned with free enzymes [4]).

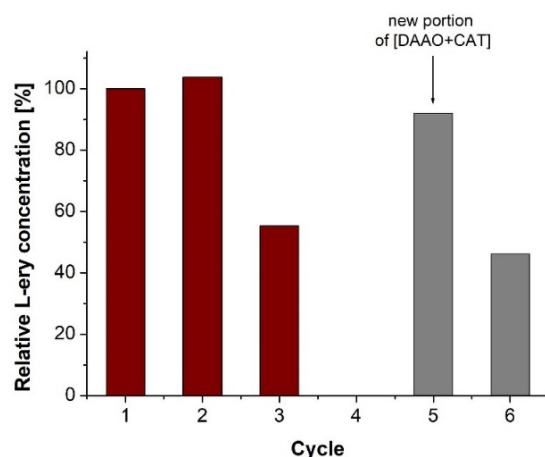


Figure 6. Recycling of co-immobilized [DAAO+CAT][TK] at 30 °C. Conditions: D-serine (50 mM), GOA (50 mM), ThDP (0.1 mM), MgCl₂ (1 mM), 0.5 g of [DAAO+CAT] biocatalyst with immobilized 2 mg of DAAO_{Rg} and 4 mg of CAT and 0.5 g of [TK] biocatalyst with immobilized 6 mg of TK_{gst} pH 7.0, 30 °C, 400 rpm, in the presence of O₂, pH regulated by pH-stat, after 4th cycle, a new portion of co-immobilized DAAO_{Rg} (2 mg) and CAT (4 mg) was added. The enzyme activity after the 1st cycle is 100%.

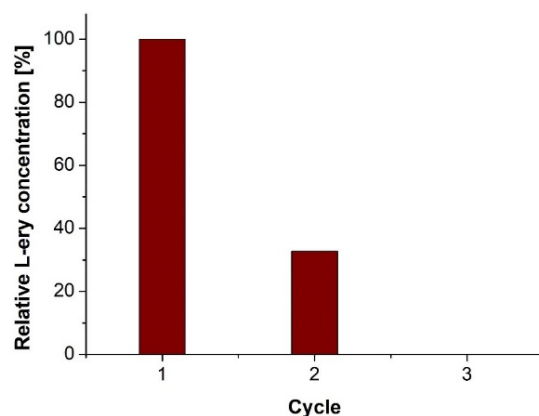


Figure 7. Recycling of co-immobilized [DAAO+CAT+TK] at 30 °C. Conditions: D-serine (50 mM), GOA (50 mM), ThDP (0.1 mM), MgCl_2 (1 mM), 1 g of [DAAO+CAT+TK] biocatalyst with immobilized 2 mg of DAAO_{Rg} and 6 mg of TK_{gst} , and 4 mg of CAT, pH 7.0, 30 °C, 400 rpm, in the presence of O_2 , 6 h of reaction time for each cycle. The enzyme activity after the 1st cycle is 100%.

This hypothesis was supported by the absence of HPA formation observed by HPLC in the subsequent reaction cycles. Therefore, the introduction of a new portion of [DAAO+CAT] in the reaction mixture increased the production of L-erythrulose at a level close to that obtained after the first cycle (Figure 6). Hence, to avoid the inhibition of GOA, the process could be optimized by introducing the GOA portion-wise.

3. Materials and Methods

3.1. General

All chemicals were purchased from Sigma-Aldrich (Poznan, Poland), Alfa-Aesar (Poznan, Poland) and CarboSynth (Poznan, Poland). Bradford reagent was from Bio-Rad (Paris, France). Ni-NTA resin was obtained from QIAGEN (Les Ulis, France). Proteins and enzymes were acquired from Sigma-Aldrich. Lyophilization was carried out with a Triad LABCONCO dryer. UV-visible absorbance was measured using a Spark control 10 microplate reader from TECAN (Lyon, France) and an Agilent Technologies (Les Ulis, France), Cary 300 UV-Vis spectrophotometer enabling Peltier temperature control. MARCHEREY-NAGEL GmbH & Co KG (Düren, Germany) 60/40-63 mesh silica gel for liquid flash chromatography and MARCHEREY-NAGEL GmbH & Co KG 60 F254 silica gel TLC plates with anisaldehyde stain for detection were used. The reaction pH for preparative synthesis was maintained using a TitroLine[®]7000 autotitrator. NMR spectra were recorded in D_2O or DMSO on a 400 MHz Bruker Avance III HD spectrometer. Chemical shifts are referenced to the residual solvent peak. The following multiplicity abbreviations were used: (s) singlet, (d) doublet, (t) triplet, (m) multiplet.

3.2. Expression of TK_{gst} from *Geobacillus stearothermophilus* and DAAO_{Rg} from *Rhodotorula gracilis*

Escherichia coli strain BL21(DE3)pLysS was used for wild-type TK_{gst} [14,15], overexpression with the plasmid pET47b and for DAAO_{Rg} overexpression [41] with the plasmid pT7. These strains were stored at -80 °C in glycerol (10%). One colony of each recombinant *E. coli* strain, grown on selective LB agar plates, was transferred into 30 mL liquid Lurica-Bertani medium containing ampicillin ($100 \mu\text{g}\cdot\text{mL}^{-1}$) or kanamycin ($30 \mu\text{g}\cdot\text{mL}^{-1}$) and grown at 37 °C, 130 rpm for 12 h. A total of 20 mL of the pre-culture was used to inoculate 1 L of culture medium containing ampicillin ($100 \mu\text{g}\cdot\text{mL}^{-1}$) or kanamycin ($30 \mu\text{g}\cdot\text{mL}^{-1}$) and grown at 37 °C, 200 rpm. Isopropyl β -D-1-thiogalactopyranoside (IPTG) at 0.5 mM was added when the $\text{OD}_{600\text{nm}}$ range was 0.7–0.8. The cells were then grown overnight at 30 °C, with stirring at 130 rpm, and harvested by centrifuging at 8000 rpm at 4 °C for 15 min. Bacterial pellets were washed twice with phosphate buffer ($\text{NaH}_2\text{PO}_4\cdot 2\text{H}_2\text{O}$, 50 mM), NaCl (300 mM, pH 8.0) and harvested (≈ 5 g/L for TKs and ≈ 2 g/L for DAAO_{Rg}).

3.3. Purification of TK_{gst} and $DAAO_{Rg}$

Harvested recombinant cells from 1 L of culture were resuspended in 35 mL of phosphate buffer (50 mM) containing NaCl (300 mM) at pH 8.0 for TKs and 14 mL of phosphate buffer (50 mM) containing 2-mercaptoethanol (5 mM) and FAD (0.1 mM) at pH 7.2 for $DAAO_{Rg}$ [45]. The cells were disrupted by sonication on ice for 30 min and the insoluble pellets were discarded after centrifuging at 8000 rpm for 15 min at 4 °C. Crude extracts were applied to a Ni-NTA column equilibrated with phosphate buffer for TK_{gst} and with phosphate buffer (50 mM) containing NaCl (1 M), imidazole (20 mM) and glycerol 5% at pH 7.2 for $DAAO_{Rg}$. After washing each column with the same buffer for TKs and $DAAO_{Rg}$, respectively, the His6-tagged TKs or $DAAO_{Rg}$ were finally eluted with phosphate buffer (50 mM) containing NaCl (300 mM) and imidazole (500 mM) at pH 8.0 for TKs and phosphate buffer (50 mM) containing glycerol (5%) imidazole (50 mM) at pH 7.2 for $DAAO_{Rg}$. The fractions containing the eluted proteins were collected and dialyzed against triethanolamine buffer (2 mM, pH 7.5) and then against water (pH 7.5) through dialysis tubing (cut-off 14 kDa) at 4 °C for TKs and twice against water (pH 7.5) through dialysis tubing at 4 °C for $DAAO_{Rg}$. These protein solutions were then lyophilized. Protein concentration was determined through the Bradford method [46] and bovine serum albumin (BSA) was used as the standard. The specific activities of lyophilized TK_{gst} , and $DAAO_{Rg}$ were 21 U, and 37 U per mg of total protein, respectively, at 25 °C. The purity and molecular mass of these samples were analysed by SDS-PAGE [4,36] using Precision Plus Protein™ All Blue Standards#161-0373 (10–250 kDa, Bio-Rad) as standard. The proteins were visualized with Coomassie Blue G-250.

3.4. Synthesis and Functionalization of Silica Monoliths (MH)

The MH was synthesized and functionalized with amino groups using a method described in detail earlier [26,28].

3.5. Immobilization of Enzymes on Amino-Modified MH

Before immobilization, the amino modified MH were washed with ethanol, distilled water, and phosphate buffer (0.1 M, pH 7.0, Na_2HPO_4/KH_2PO_4). The amino groups have to be activated with glutaraldehyde before enzyme addition—the MH were incubated with glutaraldehyde (GLA) solution (2.5% (v/v) in phosphate buffer (0.1 M, pH 7.0) for 2 h. Next, excess GLA was eluted with distilled water and phosphate buffer (0.1 M, pH 7.0). For single enzyme immobilization ([$DAAO$] or [CAT] or [TK]), to the MH carriers, enzyme solution in phosphate buffer (0.1 M, pH 7.0, Na_2HPO_4/KH_2PO_4) was added and incubated for 3 h, at RT and then at 6 °C overnight. For [$DAAO$ +CAT] co-immobilization, the MH was first immersed in $DAAO_{Rg}$ solution for 2 h, at RT, CAT solution was then added, and the whole was incubated for the next 2 h, and then left at 6 °C overnight. For [$DAAO$ +CAT+TK] co-immobilization, MH was first immersed in TK_{gst} solution. $DAAO_{Rg}$ solution was then added, followed by CAT solution. After each enzyme addition, 2 h incubation at RT was carried out. Finally, they were left at 6 °C overnight. Excess protein in all cases was removed by washing, as described elsewhere [26,28,47]. The amount of immobilized enzymes was calculated as the difference between the enzyme given to immobilization (mg) and the enzyme eluted (mg) divided by the amount of carriers given for immobilization (g). The concentration of enzymes was determined using the Lowry method (Sigma-Aldrich).

3.6. Activity of Single Immobilized $DAAO_{Rg}$

The activity of immobilized $DAAO_{Rg}$ was determined in the presence of D-serine (D-ser) giving HPA and H_2O_2 . Catalase (CAT) is essential for $DAAO_{Rg}$ enzyme protection and allows for dismutation of H_2O_2 to H_2O and O_2 . Unless stated otherwise, D-serine (50 mM) was dissolved in Tris-HCl buffer (0.5 M, pH 7.0). The reaction mixture was incubated for 10 min at 26 °C. Native catalase and immobilized $DAAO_{Rg}$ were then added. The reaction was carried out at the same temperature and samples were taken after 3, 5, and 12 min. The amount of HPA produced was checked by the HPLC method

described below. All measurements were performed in triplicate using basket stationary bed reactor StatBioChem.

3.7. Activity of Single Immobilized TK_{gst}

The activity of immobilized TK_{gst} was specified in the synthesis of L-erythrulose from hydroxypyruvate (HPA) and glycoaldehyde (GOA). Unless stated otherwise, HPA (50 mM) and GOA (50 mM), with ThDP (0.1 mM) and $MgCl_2$ (1 mM) as cofactors, were dissolved in distilled water and the pH was adjusted to 7.0 with 0.1 M NaOH. The reaction mixture was then first incubated at different temperatures for 15 min and then the enzyme was added. The reaction was carried out at the same temperature and samples were taken after 1, 3, and 5 min. The amount of L-erythrulose obtained was determined by the HPLC method described below. All measurements were performed in triplicate using basket stationary bed reactor StatBioChem.

3.8. L-Erythrulose Synthesis by Immobilized $DAAO_{Rg}$, TK_{gst} , and CAT

The general procedure is described elsewhere [4]. In short, D-serine (50 mM), GOA (50 mM), ThDP (0.1 mM), and $MgCl_2$ (1 mM) were dissolved in H_2O , the pH was adjusted to 7.0 with 0.1 M NaOH, and the reaction mixture was incubated at 30 °C for 10 min. The immobilized enzymes were then added [$DAAO+CAT+TK$] or [$DAAO+CAT$][TK] or [$DAAO$][CAT][TK]. Oxygen was bubbled into the reactor (10 mL/min). The reaction mixture was stirred (400 rpm) at 30 °C and the pH was automatically maintained at 7 by adding 0.1 M HCl using a pH-stat. Reaction progress as a L-erythrulose synthesis was followed by the HPLC method described below.

3.9. Determination of HPA, Glycolaldehyde, and L-Erythrulose Concentration

Quantitative analysis of the reaction mixture containing HPA, GOA, and L-erythrulose was performed by HPLC (Agilent 1200 series) equipped with a Bio-Rad Aminex HPX-87H column (300 × 7.8 mm) at 60 °C and 0.1% TFA in water as a mobile phase. A 10 µL aliquot of sample was injected into the HPLC operating at a flow rate of 0.6 mL/min. Substrates and products were detected using a refractive index (RI) detector.

4. Conclusions

This work shows that $DAAO_{Rg}$ and TK_{gst} were efficiently immobilized by covalent bonds on monolithic silica supports. Immobilization improved the long-term stability of enzymes in water at increasing temperatures and allowed their repeated usage (five-fold reusability of each immobilized enzyme) without loss of activity. A cascade reaction was developed and performed in a basket reactor using D-serine and GOA as substrates. Three immobilization strategies of $DAAO_{Rg}$, CAT, and TK_{gst} were tested, and it was shown that the best L-erythrulose concentration (61% of L-erythrulose yield) was obtained when $DAAO_{Rg}/CAT$ were immobilized together and TK_{gst} separately. This result highlights the expected substrate channelling effect, allowing a direct H_2O_2 consumption by CAT, and so avoiding its destructive effect on $DAAO_{Rg}$ activity. The joint or separate immobilization of TK_{gst} with [$DAAO+CAT$] ([$DAAO+CAT+TK$] or [$DAAO+CAT$][TK], respectively) did not greatly change L-erythrulose yield, which in turn could be due to the open pore structure of the silica support. It may therefore be assumed that efficient substrate channelling is particularly important for eliminating enzyme-destructive reagents, such as H_2O_2 . The best reusability was obtained with [$DAAO+CAT$][TK], producing the same amount of L-erythrulose formation after two cycles. L-erythrulose synthesis could be optimized by introducing GOA dropwise to circumvent the inhibition of $DAAO_{Rg}$ by GOA and a higher amount of CAT could be immobilized on the support to obtain a more efficient H_2O_2 dismutation. This process could be also applied to the synthesis of a wide range of α -hydroxyketones from D-serine and suitable aldehydes as already described with free enzymes. In addition, the combination of [$DAAO+CAT$][TK] could offer the advantage to replace TK with other enzyme(s) extending the potentialities of this strategy.

Supplementary Materials: The following supporting information can be downloaded at: <https://www.mdpi.com/article/10.3390/catal13010095/s1>. Figure S1. Long-term thermal stability of free and immobilized DAAO_{RG} and TK_{gst}. Table S1. Structure parameters of silica monolithic beads before and after functionalization with amino groups.

Author Contributions: D.Ś., investigation, methodology, and writing—original draft preparation; A.Ł., investigation; N.O., investigation and methodology; L.P., writing—review and editing; F.C.—writing—review and editing; L.H., writing—review and editing, conceptualization, and funding acquisition; K.S., conceptualization, writing—original draft preparation, and writing—review and editing, supervision. All authors have read and agreed to the published version of the manuscript.

Funding: This project was financed by the National Science Centre of Poland (NCN) under grant UMO-2016/23/B/ST8/00627 and by ERA CoBioTech TRALAMINOL—ID: 64 (grant to L.H.).

Institutional Review Board Statement: Not applicable.

Informed Consent Statement: Not applicable.

Data Availability Statement: Not applicable.

Conflicts of Interest: There are no conflict to declare.

References

- Chen, Z.; Li, Z.; Li, F.; Wang, M.; Wang, N.; Gao, X.-D. Cascade synthesis of rare ketoses by whole cells based on l-rhamnulose-1-phosphate aldolase. *Enzyme Microb. Technol.* **2020**, *133*, 109456. [CrossRef]
- Li, Z.; Li, F.; Cai, L.; Chen, Z.; Qin, L.; Gao, X.-D. One-Pot Multienzyme Synthesis of Rare Ketoses from Glycerol. *J. Agric. Food Chem.* **2020**, *68*, 1347–1353. [CrossRef]
- Ocal, N.; L'enfant, M.; Charmantray, F.; Pollegioni, L.; Martin, J.; Auffray, P.; Collin, J.; Hecquet, L. D-serine as a Key Building block: Enzymatic process development and smart applications within the cascade enzymatic concept. *Org. Proces. Res. Dev.* **2020**, *24*, 769–775. [CrossRef]
- L'enfant, M.; Bruna, F.; Lorilliere, M.; Ocal, N.; Fessner, W.-D.; Pollegioni, L.; Charmantray, F.; Hecquet, L. One-pot cascade synthesis of (3S)-hydroxyketones catalyzed by transketolase via hydroxypyruvate generated in situ from D-serine by D-amino acid oxidase. *Adv. Synth. Catal.* **2019**, *361*, 2550–2558. [CrossRef]
- Lorilliere, M.; De Sousa, M.; Bruna, F.; Heuson, E.; Gefflaut, T.; de Berardinis, V.; Saravanan, T.; Yi, D.; Fessner, W.-D.; Charmantray, F.; et al. One-pot, two-step cascade synthesis of naturally rare L-erythro (3S,4S) ketoses by coupling a thermostable transaminase and transketolase. *Green Chem.* **2017**, *19*, 425–435. [CrossRef]
- Zhong, C.; Duić, B.; Bolivar, J.M.; Nidetzky, B. Three-Enzyme Phosphorylase Cascade Immobilized on Solid Support for Biocatalytic Synthesis of Cellooligosaccharides. *ChemCatChem* **2020**, *12*, 1350–1358. [CrossRef]
- Kumpf, A.; Kowalczykiewicz, D.; Szymańska, K.; Mehnert, M.; Bento, I.; Łochowicz, A.; Pollender, A.; Jarzębski, A.; Tischler, D. Immobilization of the Highly Active UDP-Glucose Pyrophosphorylase from *Thermococcus agrestis* Provides a Highly Efficient Biocatalyst for the Production of UDP-Glucose. *Front. Bioeng. Biotechnol.* **2020**, *8*, 740. [CrossRef] [PubMed]
- Stradowska, D.; Heba, M.; Czernek, A.; Kuźnik, N.; Gillner, D.; Maresz, K.; Pudło, W.; Jarzębski, A.; Szymańska, K. Lipase immobilized on MCFs as biocatalysts for kinetic and dynamic kinetic resolution of *sec*-alcohols. *Catalysts* **2015**, *11*, 518. [CrossRef]
- Kuan, I.; Liao, R.; Hsieh, H.; Chen, K.; Yu, C. Properties of *Rhodotorula gracilis* d-Amino Acid Oxidase Immobilized on Magnetic Beads through His-Tag. *J. Biosci. Bioeng.* **2008**, *105*, 110–115. [CrossRef]
- Wang, M.; Qi, W.; Xu, H.; Yu, H.; Zhang, S.; Shen, Z. Affinity-binding immobilization of d-amino acid oxidase on mesoporous silica by a silica-specific peptide. *J. Ind. Microbiol. Biotech.* **2019**, *46*, 1461–1467. [CrossRef] [PubMed]
- Li, R.; Sun, J.; Fu, Y.; Du, K.; Cai, M.; Ji, P.; Feng, W. Immobilization of genetically-modified D-amino acid oxidase and catalase on carbon nanotubes to improve the catalytic efficiency. *Catalysts* **2016**, *6*, 66. [CrossRef]
- Dang, P.T.; Le, H.G.; Hoang, V.T.; Tran, H.T.H.; Dao, C.D.; Nguyen, K.T.; Le, G.H.; Nguyen, Q.K.; Nguyen, T.V.; Vu, T.A. Immobilization of D-amino acid oxidase enzyme on hybrid mesoporous MCF, SBA-15 and MCM-41 nanomaterials. *J. Nanosci. Nanotechnol.* **2017**, *7*, 947–953. [CrossRef] [PubMed]
- Matosevic, S.; Lye, G.J.; Baganz, F. Design and Characterization of a Prototype Enzyme Microreactor: Quantification of Immobilized Transketolase Kinetics. *Biotechnol. Prog.* **2010**, *26*, 118–126. [CrossRef] [PubMed]
- Benaissi, K.; Helaine, V.; Prevot, V.; Forano, C.; Hecquet, L. Efficient Immobilization of Yeast Transketolase on Layered Double Hydroxides and Application for Ketose synthesis. *Adv. Synth. Catal.* **2011**, *353*, 1497–1509. [CrossRef]
- Ali, G.; Moreau, T.; Forano, C.; Mousty, C.; Prevot, V.; Charmantray, F.; Hecquet, L. Chiral polyol synthesis catalyzed by a thermostable Transketolase immobilized on Layered Double Hydroxides in Ionic liquids. *ChemCatChem* **2015**, *7*, 3163–3170. [CrossRef]
- Xu, K.; Chen, X.; Zheng, R.; Zheng, Y. Immobilization of Multi-Enzymes on Support Materials for Efficient Biocatalysis. *Front. Bioeng. Biotechnol.* **2020**, *8*, 660. [CrossRef]

17. Arana-Pena, S.; Carballares, D.; Morellon-Sterling, R.; Berenguer-Murcia, A.; Alcantara, A.R.; Rodrigues, R.C.; Fernandez-Lafuente, R. Enzyme co-immobilization: Always the biocatalyst designers' choice . . . or not? *Biotechnol. Adv.* **2021**, *51*, 107584. [[CrossRef](#)]
18. Bilal, M.; Hussain, N.; Americo-Pinheiro, J.H.P.; Almulaiky, Y.Q.; Iqbal, H.M.N. Multi-enzyme co-immobilized nano-assemblies: Bringing enzymes together for expanding bio-catalysis scope to meet biotechnological challenges. *Int. J. Biol. Macromol.* **2021**, *186*, 735–749. [[CrossRef](#)]
19. Hwang, E.T.; Lee, S. Multienzymatic Cascade Reactions via Enzyme Complex by Immobilization. *ACS Catal.* **2019**, *9*, 4402–4425. [[CrossRef](#)]
20. Ren, S.; Li, C.; Jiao, X.; Jia, S.; Jiang, Y.; Bilal, M.; Cui, J. Recent progress in multienzymes co-immobilization and multienzyme system applications. *Chem. Eng. J.* **2019**, *373*, 1254–1278. [[CrossRef](#)]
21. Sanchez- Otero, M.G.; Quintana-Castro, R.; Rojas-Vazquez, A.S.; Badillo-Zeferino, G.L.; Mondragón-Vazquez, K.; Espinosa-Luna, G.; Nadda, A.K.; Oliart-Ros, R.M. Polypropylene as a selective support for the immobilization of lipolytic enzymes: Hyper-activation, purification and biotechnological applications. *J. Chem. Technol. Biotechnol.* **2022**, *97*, 436–445. [[CrossRef](#)]
22. Rather, H.; Khan, R.S.; Wani, T.U.; Beigh, M.A.; Sheikh, F.A. Overview on immobilization of enzymes on synthetic polymeric nanofibers fabricated by electrospinning. *Biotechnol. Bioeng.* **2022**, *119*, 9–23. [[CrossRef](#)]
23. Singh, A.; Rai, S.K.; Manisha, M.; Yadav, S.K. Immobilized L-ribose isomerase for the sustained synthesis of a rare sugar D-talose. *Mol. Catal.* **2021**, *511*, 11723. [[CrossRef](#)]
24. Gentil, S.; Pifferi, C.; Rousselot-Pailley, P.; Tron, T.; Renaudet, O.; Le Goff, A. Clicked Bifunctional Dendrimeric and Cyclopeptidic Addressable Redox Scaffolds for the Functionalization of Carbon Nanotubes with Redox Molecules and Enzymes. *Langmuir* **2021**, *37*, 1001–1011. [[CrossRef](#)] [[PubMed](#)]
25. Cristovao, R.O.; Almeida, M.R.; Barros, M.A.; Nunes, J.C.F.; Boaventura, R.A.R.; Loureiro, J.M.; Faria, J.L.; Neves, M.C.; Freire, M.G.; Ebinuma-Santos, V.C.; et al. Development and characterization of a novel L-asparaginase/MWCNT nanobioconjugate. *RSC Adv.* **2020**, *10*, 31205. [[CrossRef](#)] [[PubMed](#)]
26. Szymańska, K.; Odrozek, K.; Zniszczoł, A.; Pudło, W.; Jarzębski, A. A novel hierarchically structured siliceous packing to boost the performance of rotating bed enzymatic reactors. *Chem. Eng. J.* **2017**, *315*, 18–24. [[CrossRef](#)]
27. Hou, C.; Ghéczy, N.; Messmer, D.; Szymańska, K.; Adamcik, J.; Mezzenga, R.; Jarzębski, A.B.; Walde, P. Stable immobilization of enzymes in a macro- and mesoporous silica monolith. *ACS Omega* **2019**, *4*, 7795–7806. [[CrossRef](#)]
28. Kowalczykiewicz, D.; Szymańska, K.; Gillner, D.; Jarzębski, A.B. Rotating bed reactor packed with heterofunctional structured silica-supported lipase. Developing an effective system for the organic solvent and aqueous phase reactions. *Microporous Mesoporous Mater.* **2021**, *312*, 110789. [[CrossRef](#)]
29. Butò, S.; Pollegioni, L.; D'Angiuro, L.; Pilone, M.S. Evaluation of D-amino acid oxidase from *Rhodotorula gracilis* for the production of α -keto acids: A reactor system. *Biotechnol. Bioeng.* **1994**, *44*, 1288–1294. [[CrossRef](#)]
30. Sun, J.; Du, K.; Song, X.; Gao, Q.; Wu, H.; Ma, J.; Ji, P.; Feng, W. Specific immobilization of D-amino acid oxidase on hematin functionalized support mimicking multi enzyme catalysis. *Green Chem.* **2015**, *17*, 4465. [[CrossRef](#)]
31. Ranoux, A.; Karmee, S.K.; Jin, J.; Bhaduri, A.; Caiazzo, A.; Arends, I.W.; Hanefeld, U. Enhancement of the Substrate Scope of Transketolase. *ChemBioChem.* **2012**, *13*, 1921–1931. [[CrossRef](#)]
32. Subrizi, F.; Cárdenas-Fernández, M.; Lye, G.J.; Ward, J.M.; Dalby, P.A.; Sheppard, T.D.; Hailes, H.C. Transketolase catalysed upgrading of l-arabinose: The one-step stereoselective synthesis of l-gluco-heptulose. *Green Chem* **2016**, *18*, 3158–3165. [[CrossRef](#)]
33. Bawn, M.; Subrizi, F.; Lye, G.J.; Sheppard, T.D.; Hailes, H.C.; Ward, J.M. One-pot, two-step transaminase and transketolase synthesis of l-gluco-heptulose from l-arabinose. *Enzyme Microb. Technol.* **2018**, *116*, 16–22. [[CrossRef](#)] [[PubMed](#)]
34. James, P.; Isupov, M.N.; De Rose, S.A.; Sayer, C.; Cole, I.S.; Littlechild, J.A. A 'Split-Gene' Transketolase from the Hyper-Thermophilic Bacterium *Carboxydothermus hydrogenoformans*: Structure and Biochemical Characterization. *Front. Microbiol.* **2020**, *11*, 592353. [[CrossRef](#)]
35. Cardenas-Fernandez, M.; Subrizi, F.; Dobrijevic, D.; Hailes, H.C.; Ward, J.M. Characterisation of a hyperthermophilic transketolase from *Thermotoga maritima* DSM3109 as a biocatalyst for 7-keto-octuronic acid synthesis. *Org. Biomol. Chem.* **2021**, *19*, 6493–6500. [[CrossRef](#)]
36. Abdoul Zabar, J.; Sorel, I.; Helaine, V.; Charmantray, F.; Devamani, T.; Yi, D.; de Berardinis, V.; Louis, D.; Marilere, P.; Fessner, W.D.; et al. Thermostable transketolase from *Geobacillus stearothermophilus*: Characterization and catalytic properties. *Adv. Synth. Catal.* **2013**, *355*, 116–128. [[CrossRef](#)]
37. Lorillière, M.; Dumoulin, R.; L'Enfant, M.; Rambourdin, A.; Thery, V.; Nauton, L.; Fessner, W.D.; Charmantray, F.; Hecquet, L. Evolved Thermostable Transketolase for Stereoselective Two-Carbon Elongation of Non-Phosphorylated Aldoses to Naturally Rare Ketoses. *ACS Catal.* **2019**, *9*, 4754–4763. [[CrossRef](#)]
38. Szymańska, K.; Pietrowska, M.; Kocurek, J.; Maresz, K.; Koreniuk, A.; Mrowiec-Białoń, J.; Widlak, P.; Magner, E.; Jarzębski, A. Low back-pressure hierarchically structured multichannel microfluidic bioreactors for rapid protein digestion—Proof of concept. *Chem. Eng. J.* **2016**, *287*, 148–154. [[CrossRef](#)]
39. Nezhad, M.K.; Aghaei, H. Tosylated cloisite as a new heterofunctional carrier for covalent immobilization of lipase and its utilization for production of biodiesel from waste frying oil. *Renew. Energy* **2019**, *275*, 95–104. [[CrossRef](#)]
40. Bedade, D.K.; Sutar, Y.B.; Singhal, R.S. Chitosan coated calcium alginate beads for covalent immobilization of acrylamidase: Process parameters and removal of acrylamide from coffee. *Food Chem.* **2019**, *275*, 95–104. [[CrossRef](#)]

41. Pollegioni, L.; Falbo, A.; Pilone, M.S. Specificity and kinetics of *Rhodotorula gracilis* d-amino acid oxidase. *Biochem. Biophys. Acta* **1992**, *1120*, 11–16. [[CrossRef](#)] [[PubMed](#)]
42. Groth, L. Heat and pH dependence of catalase. A comparative study. *Acta Biol. Hung.* **1987**, *38*, 279–285.
43. Alptekin, O.; Seyhan Tukel, S.; Yildirim, D. Immobilization and characterization of bovine liver catalase on eggshell. *J. Serb. Chem. Soc.* **2008**, *73*, 609–618. [[CrossRef](#)]
44. Mathesh, M.; Liu, J.; Barrow, C.J.; Yang, W. Graphene-Oxide-Based Enzyme Nanoarchitectonics for Substrate Channeling. *Chem. Eur. J.* **2016**, *23*, 304–311. [[CrossRef](#)] [[PubMed](#)]
45. Fantinato, S.; Pollegioni, L.; Pilone, M.S. Engineering, expression and purification of his-tagged chimeric D-amino acid oxidase from *Rhodotorula gracilis*. *Enzyme Microb. Technol.* **2001**, *29*, 407–412. [[CrossRef](#)]
46. Bradford, M.M. A rapid and sensitive method for the quantitation of microgram quantities of protein utilizing the principle of protein-dye binding. *Anal. Biochem.* **1976**, *72*, 248–254. [[CrossRef](#)]
47. Kowalczykiewicz, D.; Przypis, M.; Mestrom, L.; Kumpf, A.; Tischler, D.; Hagedoorn, P.L.; Hanefeld, U.; Jarzębski, A.; Szymańska, K. Engineering of continuous bienzymatic cascade process using monolithic microreactors—In flow synthesis of trehalose. *Chem. Eng. J.* **2022**, *427*, 131439. [[CrossRef](#)]

Disclaimer/Publisher’s Note: The statements, opinions and data contained in all publications are solely those of the individual author(s) and contributor(s) and not of MDPI and/or the editor(s). MDPI and/or the editor(s) disclaim responsibility for any injury to people or property resulting from any ideas, methods, instructions or products referred to in the content.